K1:01 K1:02

Infinitesimally Locked Self-Touching Linkages with Applications to Locked Trees

K1:03 Robert Connelly, Erik D. Demaine, and Günter Rote

Abstract. Recently there has been much interest in linkages (bar-and-joint frameworks) that are *locked* or *stuck* in the sense that they cannot be moved into some other configuration while preserving the bar lengths and not crossing any bars. We propose a new algorithmic approach for analyzing whether planar linkages are locked in many cases of interest. The idea is to examine *self-touching* or *degenerate* frameworks in which multiple edges converge to geometrically overlapping configurations. We show how to study whether such frameworks are locked using techniques from rigidity theory, in particular first-order rigidity and equilibrium stresses. Then we show how to relate locked self-touching frameworks to locked frameworks that closely approximate the self-touching frameworks. Our motivation is that most existing approaches to locked linkages are based on approximations to self-touching frameworks. In particular, we show that a previously proposed locked tree in the plane [**BDD$^+$02**] can be easily proved locked using our techniques, instead of the tedious arguments required by standard analysis. We also present a new locked tree in the plane with only one degree-3 vertex and all other vertices degree 1 or 2. This tree can also be easily proved locked with our methods, and implies that the result about opening polygonal arcs and cycles [**CDR02**] is the best possible.

K1:04

1. Linkages

K1:05 K1:06 K1:07 K1:08 K1:09 K1:10 K1:11 K1:12 K1:13 K1:14 K1:15 K1:16 K1:17 K1:18

A *linkage* is a graph together with an assignment of lengths to edges; each edge is called a rigid *bar*. We highlight three linkages of common study: a *polygonal arc*, *polygonal cycle*, or *polygonal tree* is a linkage whose graph is a single path, cycle, or tree, respectively. A *configuration* of a linkage in $\mathbb{R}^d$ is a mapping of the vertices to points in $\mathbb{R}^d$ that satisfies the bar-length constraints. A configuration is (*strongly*) *simple* if only incident bars intersect, and then only at the common endpoint. A *motion* is a continuum of configurations, that is, a continuous function mapping the time interval $[0, 1]$ to configurations; often, each configuration is required to be simple. The *configuration space* of a given subset of configurations (e.g., simple configurations) is the space in which points correspond to configurations and paths correspond to motions.

We focus here on *planar linkages* embedded in $\mathbb{R}^2$. In this case, the linkage also specifies the combinatorial planar embedding because this cannot change by a motion that avoids crossings. It is known that the configuration space of simple

K1:19

2000 *Mathematics Subject Classification.* Primary: 52C25.

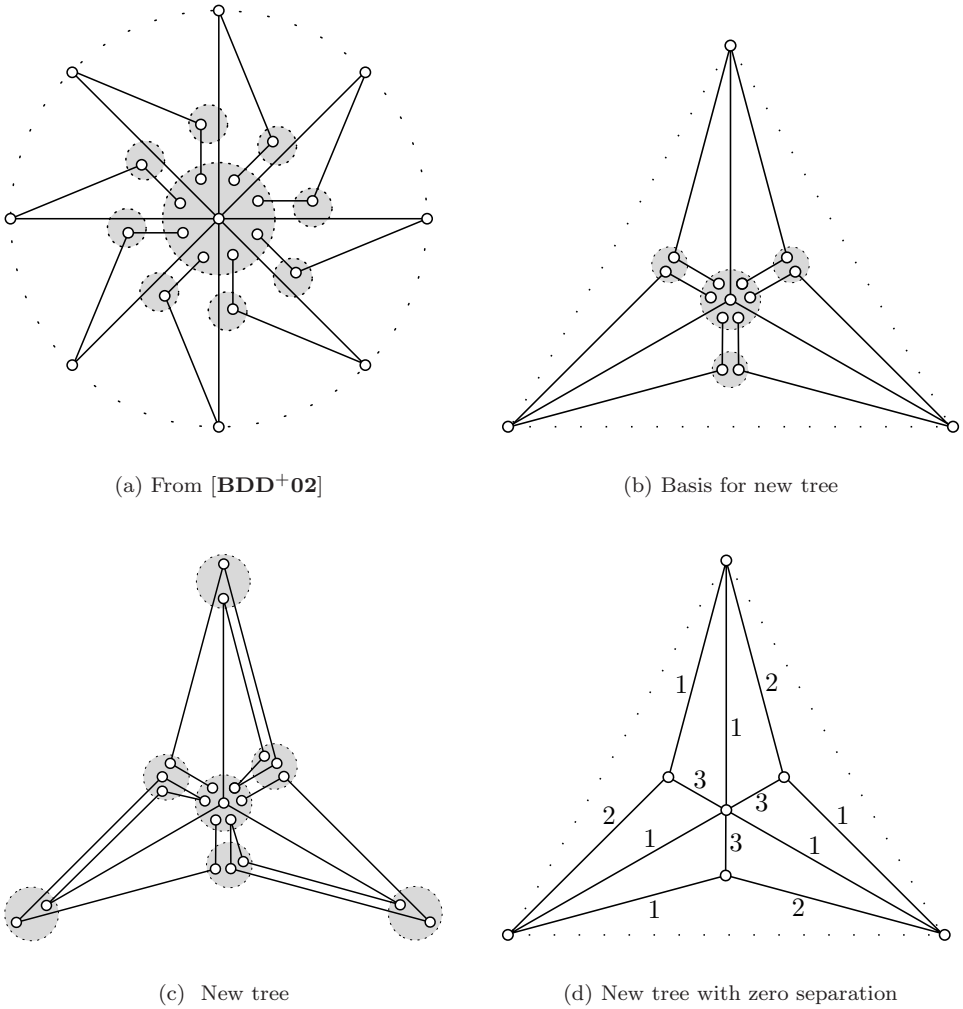

(a) From [**BDD$^+$02**]

(b) Basis for new tree

(c) New tree

(d) New tree with zero separation

FIGURE 1. Locked planar polygonal trees. Points in dotted circles are closer than they appear.

K2:01 planar configurations is not always connected for a polygonal tree, as exemplified
K2:02 by the pinwheel tree in Figure 1(a) [**BDD$^+$02**], and is always connected for a
K2:03 polygonal arc, polygonal cycle (up to reflection), and disjoint union of nonnested
K2:04 polygonal arcs and cycles [**CDR02, Str00**]. The key distinction is that arcs and
K2:05 cycles have maximum degree 2, but a tree may have vertices of higher degree.
K2:06 See [**CDR02, Dem00, O'R98**] for surveys of related results.

K2:07 Two questions naturally arise from these results.

K2:08 First, how many high-degree vertices are necessary, and how high must the
K2:09 degrees be, to make a tree have a disconnected configuration space? For example,
K2:10 the pinwheel tree in Figure 1(a) can be made to have a single degree-5 vertex, or
K2:11 three degree-3 vertices [**BDD$^+$02**]. We settle this question by proving that the

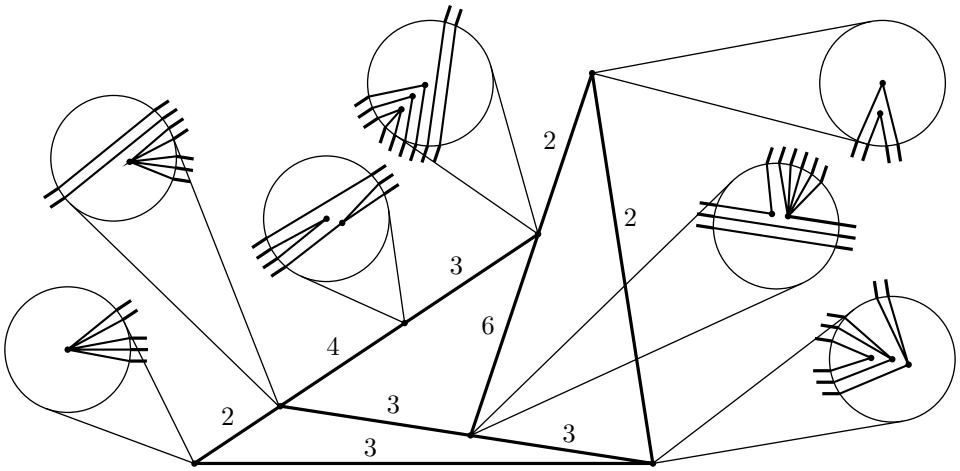

FIGURE 2. A self-touching linkage with 14 vertices and 21 edges. Numbers denote edge multiplicities.

K3:01 maximum-degree-2 result [**CDR02**] is tight: a single degree-3 vertex can prevent
K3:02 opening. See Figures 1(b) and 1(c) for the two-step construction.

K3:03 Second, and more generally, how can we tell whether a linkage has a connected
K3:04 configuration space? The best general algorithmic result for this problem is to
K3:05 use the roadmap algorithm for general motion planning [**Can87, Can88**], which
K3:06 runs in polynomial space but exponential time. We present a method for designing
K3:07 examples that can be proved without much effort to have a disconnected configura-
K3:08 tion space, and furthermore to be *strongly locked* in the sense that the tighter the
K3:09 linkage is constructed, the less freedom it has to move. This result does not settle
K3:10 the algorithmic decision problem, but solves many cases of interest. In particular,
K3:11 we use this result in our solution to the first problem.

K3:12 ## 2. Self-Touching Linkages

K3:13 Here we begin the exploration of the analogous linkage problems when bars
K3:14 are allowed to touch, and even lie along each other, but not properly cross. (A
K3:15 *proper crossing* is an intersection between the relative interiors of two nonparallel
K3:16 segments.) Our notion of self-touching linkage is an idealization because vertices
K3:17 and edges have no thickness. However, as we shall see, self-touching linkages can
K3:18 be used as a tool for studying properties of (more realistic) simple configurations
K3:19 of linkages.

K3:20 When we draw a geometric configuration of a self-touching linkage, several
K3:21 vertices and/or bars may coincide. (Such configurations are sometimes called *weakly*
K3:22 *simple*.) Thus, in addition to the geometric embedding, we require topological
K3:23 information to clarify the relationship between touching vertices and bars.

K3:24 More precisely, a *self-touching configuration* is defined as follows. We start with
K3:25 a plane straight-line graph P; see Figure 2 for an example. Each segment (edge) is
K3:26 marked with its *multiplicity*, that is, how many collinear bars lie along that segment.
K3:27 In addition, for each vertex, we add a microscopic *magnified view* enclosed by a
K3:28 circle. *Terminal points* on the boundary of the circle represent connections to the

K4:01 incident edges. Inside the circle, the terminals are connected by a plane graph, not
K4:02 necessarily drawn with straight-line edges, subject to the following rules:

K4:03 (1) Every terminal is incident to exactly one edge.
K4:04 (2) Every nonterminal vertex is incident to at least one edge.
K4:05 (3) There is at least one nonterminal vertex.
K4:06 (4) An edge may connect two terminals directly only if the terminals connect
K4:07 to two collinear segments that go in opposite directions.
K4:08 (5) All other edges must connect a terminal to a nonterminal vertex. In
K4:09 particular, no edge connects two nonterminal vertices.

K4:10 This structure specifies the combinatorial *linkage* associated with the configu-
K4:11 ration as follows. Its vertices are the nonterminal vertices in all circles. Its edges
K4:12 are the connections between those vertices; a single edge is a sequence starting
K4:13 and ending at a connection between a nonterminal and a terminal, and alternating
K4:14 between one or more additional segments and zero or more connections between
K4:15 terminals. We require in addition that the linkage has no duplicate edges.

K4:16 Figure 1(d) shows the multiplicities for the tree of Figure 1(c). We will not
K4:17 always use this representation in our figures; rather, we will use a schematic drawing
K4:18 where parallel edges are slightly separated, and dotted circles surround vertices
K4:19 that belong together in one point, as in Figure 1(c). This representation gives a
K4:20 clearer drawing of the underlying graph, and is closely linked to the concept of a
K4:21 δ-perturbation defined in Section 4 below.

K4:22 3. Self-Touching Configuration Space

K4:23 The *configuration space* is a space in which points correspond to self-touching
K4:24 configurations of a linkage as defined in the previous section, and paths correspond
K4:25 to motions of that linkage which keep edge lengths fixed and where no vertex or
K4:26 edge crosses through another edge. Before we examine the configuration space
K4:27 more carefully, note that a motion of a self-touching linkage can never change the
K4:28 *combinatorial embedding* of the linkage as a plane graph, i.e., the cyclic counter-
K4:29 clockwise sequence of edges around each vertex. (In addition, for graphs which
K4:30 are not connected, the combinatorial embedding also specifies the faces (cycles of
K4:31 edges) shared by several components.)

K4:32 The geometry of a configuration can be naturally represented by a vector $\mathbf{p} =$
K4:33 $(\mathbf{p}_1, \ldots, \mathbf{p}_n) \in \mathbb{R}^{2n}$, listing all coordinates for the n vertices in the linkage. It will
K4:34 be convenient to define the *distance* between two configurations $\mathbf{p}$ and $\mathbf{q}$ as the
K4:35 maximum Euclidean distance in the plane between corresponding points:

K4:36 $$\|\mathbf{p} - \mathbf{q}\| = \max_{1 \le i \le n} \|\mathbf{p}_i - \mathbf{q}_i\| \tag{3.1}$$

K4:37 Throughout the paper, r_0 denotes the minimum edge length, and $r_1 > 0$ is the
K4:38 minimum nonzero distance between two vertices or between a vertex and an edge,
K4:39 in a given configuration.

K4:40 A *motion* of a linkage with geometry $\mathbf{p}$ is specified by a continuous function
K4:41 $\mathbf{p}(t)$, $0 \le t \le T$ for some $T > 0$, with $\mathbf{p}(0) = \mathbf{p}$. Geometrically, such a motion must
K4:42 preserve the lengths of the bars:

K4:43 $$\|\mathbf{p}_i(t) - \mathbf{p}_j(t)\| = \|\mathbf{p}_i - \mathbf{p}_j\| \quad \text{for every bar } \{i, j\}. \tag{3.2}$$

K4:44 In addition, topologically, the relative positions of the parts of the linkage must
K4:45 remain *consistent*. For example, a vertex that touches an edge from the left side

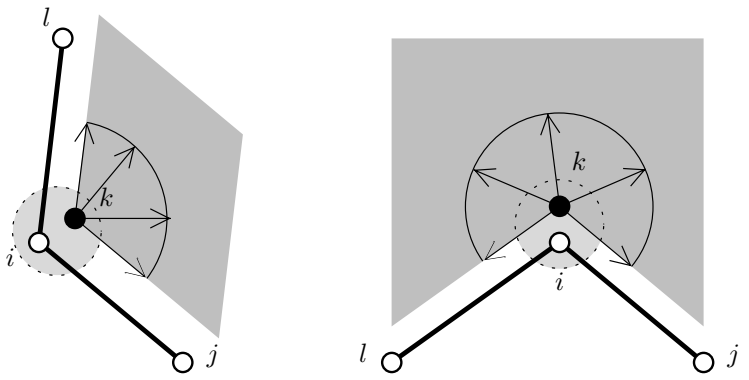

(a) Convex $\varphi \leq 180°$ (b) Reflex $\varphi > 180°$

FIGURE 3. Possible motions of vertex $\mathbf{p}_k$ (filled circle) relative to vertex $\mathbf{p}_i$ (empty circle).

K5:01 cannot suddenly move away to the right side of that edge. We shall now make
K5:02 this notion precise, and show how the set of feasible motions can be described by
K5:03 equations and inequalities, which are stable at least in some neighborhood of a given
K5:04 self-touching configuration. This development will be somewhat technical, and the
K5:05 reader who is satisfied with an intuitive understanding of self-touching linkages is
K5:06 encouraged to skip the rest of this section on first reading. The lemmas below are
K5:07 however important for the proofs in the rest of the paper.

K5:08 **3.1. Vertex-edge sidedness constraints.** First of all, we must forbid a ver-
K5:09 tex $\mathbf{p}_k$ from going through the middle of an edge $\mathbf{p}_i\mathbf{p}_j$: if $\mathbf{p}_k$ lies close to the edge
K5:10 but far enough from the endpoints $\mathbf{p}_i$ and $\mathbf{p}_j$, then $\mathbf{p}_k$ must remain on the same
K5:11 side of the edge, at least in some neighborhood of the current configuration. After
K5:12 possibly switching i and j, we can express this constraint by saying that the point
K5:13 $\mathbf{p}_k$ must remain *on the left side* of the directed line through $\mathbf{p}_i$ and $\mathbf{p}_j$ or *on* this
K5:14 line. We denote this *vertex-edge sidedness constraint* by $L(i, j; k)$. It can be written
K5:15 using the determinant expression for the signed area of the triangle $\mathbf{p}_i\mathbf{p}_j\mathbf{p}_k$:

K5:16 $$\text{area}(\triangle \mathbf{p}_i\mathbf{p}_j\mathbf{p}_k) \geq 0. \tag{3.3}$$

K5:17 Globally, we select all pairs of a vertex $\mathbf{p}_k$ and an edge $\mathbf{p}_i\mathbf{p}_j$ where the distance
K5:18 between $\mathbf{p}_k$ and the edge is at most $r_0/2$, but the distances $\|\mathbf{p}_k - \mathbf{p}_i\|$ and $\|\mathbf{p}_k - \mathbf{p}_j\|$
K5:19 are both larger than $r_0/2$. Then the side of the line $\mathbf{p}_i\mathbf{p}_j$ containing $\mathbf{p}_k$ is uniquely
K5:20 determined, and these inequalities must be fulfilled by feasible motions, as long as
K5:21 no vertex moves $r_0/4$ or more from its initial position.

K5:22 **3.2. Vertex-chain noncrossing constraints.** When $\mathbf{p}_k$ is close to an end-
K5:23 point of an edge $\mathbf{p}_i\mathbf{p}_j$, we must formulate the constraint more carefully. Suppose
K5:24 that $\mathbf{p}_k$ moves in the vicinity of $\mathbf{p}_i$. Vertex k lies in a wedge between two consecu-
K5:25 tive edges around vertex i; see Figure 3. if $\mathbf{p}_k$ is close enough to $\mathbf{p}_i$, this wedge is
K5:26 either determined by the geometry, or, if $\mathbf{p}_k = \mathbf{p}_i$, by the combinatorial information
K5:27 of the self-touching configuration.

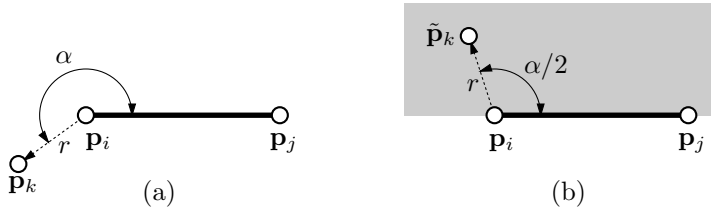

FIGURE 4. (a) The motion of $\mathbf{p}_k$ relative to $\mathbf{p}_i\mathbf{p}_j$. (b) The point $\tilde{\mathbf{p}}_k$ which is used to reparametrize the motion of $\mathbf{p}_k$, and the permitted area for $\tilde{\mathbf{p}}_k$ (shaded).

K6:01 Call the two consecutive edges of the wedge $\{j,i\}$ and $\{i,l\}$, so that vertex k
K6:02 lies in the counterclockwise wedge j,i,l. Then $\mathbf{p}_k$ is restricted to remain in this
K6:03 wedge. As a special case, vertex i may be incident to only one edge, in which case
K6:04 the two edges bounding the wedge are the same, i.e., $j = l$.

K6:05 Let us first concentrate on the motion of k relative to the edge $\mathbf{p}_i\mathbf{p}_j$. Vertex k
K6:06 can move freely but when it lies *on* the edge we must know on which side it lies.
K6:07 This cannot be distinguished on the basis of the coordinates alone. In order to
K6:08 write algebraic conditions for the feasible motions, we represent $\mathbf{p}_k$ in relative polar
K6:09 coordinates $r = \|\mathbf{p}_k - \mathbf{p}_i\|$ and the counterclockwise angle α between $\mathbf{p}_i\mathbf{p}_j$ and
K6:10 $\mathbf{p}_i\mathbf{p}_k$, $0 \le \alpha \le 2\pi$. See Figure 4. We now introduce a "shadow vertex" $\tilde{\mathbf{p}}_k = \tilde{\mathbf{p}}_{k,ij}$
K6:11 with the same distance r but with polar angle $\alpha/2$. This point is confined to the left
K6:12 half-plane of the line through $\mathbf{p}_i, \mathbf{p}_j$, disambiguating the cases $\alpha = 0$ and $\alpha = 2\pi$.

K6:13 The relation between $\tilde{\mathbf{p}}_k$ and $\mathbf{p}_k$ can be described by algebraic equations by
K6:14 using the rotation matrix $\left(\begin{smallmatrix} c & -s \\ s & c \end{smallmatrix}\right)$ with $c = \cos(\alpha/2)$ and $s = \sin(\alpha/2)$:

K6:15 $$\tilde{\mathbf{p}}_k - \mathbf{p}_i = r \begin{pmatrix} c & -s \\ s & c \end{pmatrix} (\mathbf{p}_j - \mathbf{p}_i) \cdot \frac{1}{\|\mathbf{p}_j - \mathbf{p}_i\|}$$

K6:16 $$\mathbf{p}_k - \mathbf{p}_i = r \begin{pmatrix} c & -s \\ s & c \end{pmatrix}^2 (\mathbf{p}_j - \mathbf{p}_i) \cdot \frac{1}{\|\mathbf{p}_j - \mathbf{p}_i\|}$$

K6:17 $$c^2 + s^2 = 1,\ r \ge 0,$$

K6:18 By noting that the sidedness constraint on $\tilde{\mathbf{p}}_k$ translates to $s \ge 0$ and by absorbing
K6:19 the factors r and $\frac{1}{\|\mathbf{p}_j - \mathbf{p}_i\|}$ into c and s we get the simpler parameterization

K6:20 $$\mathbf{p}_k - \mathbf{p}_i = \begin{pmatrix} a & -b \\ b & a \end{pmatrix}^2 (\mathbf{p}_j - \mathbf{p}_i), \quad a \in \mathbb{R},\ b \ge 0, \tag{3.4}$$

K6:21 using just two additional parameters a and b and eliminating $\tilde{\mathbf{p}}_k$ altogether.

K6:22 We can extend this formulation to include vertex l also and write

$$\begin{cases} \mathbf{p}_l - \mathbf{p}_i = \begin{pmatrix} \bar{a} & -\bar{b} \\ \bar{b} & \bar{a} \end{pmatrix}^2 (\mathbf{p}_j - \mathbf{p}_i) \\ \mathbf{p}_k - \mathbf{p}_i = \begin{pmatrix} a & -b \\ b & a \end{pmatrix}^2 (\mathbf{p}_j - \mathbf{p}_i) \\ a, \bar{a} \in \mathbb{R},\ b, \bar{b} \ge 0, \quad a\bar{b} \ge \bar{a}b \end{cases} \tag{3.5}$$

K6:23 using parameters $\bar{a}, \bar{b}, a, b$. The parameters $\bar{a}$ and $\bar{b}$ represent $\mathbf{p}_l$ relative to the edge
K6:24 $\mathbf{p}_i\mathbf{p}_j$ in the same way as a and b represent $\mathbf{p}_k$, and the last condition, $a\bar{b} \ge \bar{a}b$,

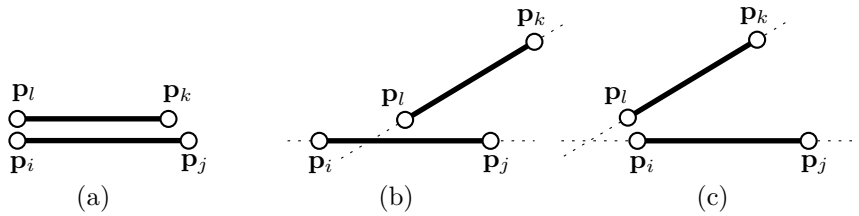

FIGURE 5. Two edges with coincident endpoints.

K7:01 essentially amounts to $a : b \geq \bar{a} : \bar{b}$, i.e., the counterclockwise angle $\mathbf{p}_j\mathbf{p}_i\mathbf{p}_k$ is
K7:02 bounded by the angle $\mathbf{p}_j\mathbf{p}_i\mathbf{p}_l$.

K7:03 The above condition remains valid as long as $\mathbf{p}_k$ does not cross the rays $\mathbf{p}_i\mathbf{p}_j$
K7:04 or $\mathbf{p}_i\mathbf{p}_l$ by going around $\mathbf{p}_j$ or $\mathbf{p}_l$.

K7:05 Globally, we look at each ordered pair of vertices i, k with $\|\mathbf{p}_i - \mathbf{p}_k\| \leq r_0/2$,
K7:06 where r_0 is the minimum edge length, and we write condition (3.5) with the four
K7:07 new parameters $a_{ik}, \bar{a}_{ik} \in \mathbb{R}$ and $b_{ik}, \bar{b}_{ik} \geq 0$. We call these conditions the *vertex-*
K7:08 *chain noncrossing conditions*. Together with the vertex-edge sidedness conditions
K7:09 (3.3), these equations and inequalities are necessary and sufficient to describe the
K7:10 motions for which no vertex moves through a chain of edges (either in the middle
K7:11 of an edge or at a vertex), as long as no vertex moves $r_0/4$ or more from its initial
K7:12 position.

K7:13 When i is incident to only one edge, or more generally, when all incident edges
K7:14 are parallel and point in the same direction, constraint (3.5) does not restrict the
K7:15 positions that $\mathbf{p}_k$ may reach, but does restrict the motions for getting there, pre-
K7:16 venting the point $\mathbf{p}_k$ from crossing these edges.

K7:17 **3.3. Edge-edge sidedness constraints.** The constraints so far still do not
K7:18 prevent an edge from moving through another edge when some endpoints of the
K7:19 two edges coincide. If two edges $\mathbf{p}_i\mathbf{p}_j$ and $\mathbf{p}_k\mathbf{p}_l$ share an endpoint $\mathbf{p}_i = \mathbf{p}_l$, as
K7:20 in Figure 5(a), they might swap sides without any vertex going through an edge.
K7:21 So we formulate an explicit sidedness condition to specify that one edge must lie
K7:22 completely on the left side of the line through the other edge:

K7:23 $$\big(L(i,j;k) \wedge L(i,j;l)\big) \vee \big(L(k,l;i) \wedge L(k,l;j)\big) \tag{3.6}$$

K7:24 The correctness of this condition can be seen by considering the possibilities how
K7:25 the lines through the two segments can intersect each other, see Figure 5(b–c). We
K7:26 call these conditions the *edge-edge sidedness conditions*.

K7:27 Again, condition (3.6) is only valid as long as the points are sufficiently close
K7:28 to the critical configuration of Figure 5(a). So we write condition (3.6) for all
K7:29 pairs of edges $\mathbf{p}_i\mathbf{p}_j$ and $\mathbf{p}_k\mathbf{p}_l$ with $\|\mathbf{p}_i - \mathbf{p}_l\| < r_0/2$ (after a suitable relabeling).
K7:30 Then, as long as no vertex moves more than $r_0/4$ from its initial position, these
K7:31 conditions (3.6) are necessary and sufficient to prevent illegal movements of the
K7:32 involved edges.

K7:33 **3.4. Local characterizations of the configuration space.** We can now
K7:34 verify that the above conditions are sufficient to characterize the feasible motions in
K7:35 some neighborhood of a given configuration. The possibilities of one vertex crossing
K7:36 through another chain of edges at the interior of an edge or at an interior vertex

K8:01 are excluded by conditions (3.3) and (3.5), respecitively. Condition (3.6) deals with
K8:02 the remaining special case of two endpoints of two chains. We summarize this
K8:03 discussion in a lemma:

K8:04 LEMMA 3.1. *Let r_0 be the minimum edge length of a self-touching linkage with*
K8:05 *coordinate vector $\mathbf{p}^*$. Consider a path $\mathbf{p}(t) \in \mathbb{R}^{2n}$, $0 \le t \le T$ with $\mathbf{p}(0) = \mathbf{p}^*$,*
K8:06 *within the $r_0/4$-neighborhood of $\mathbf{p}^*$:*

K8:07 $$\|\mathbf{p}(t) - \mathbf{p}^*\| < r_0/4, \text{ for all } 0 \le t \le T.$$

K8:08 *This path represents a feasible motion in the configuration space of self-touching*
K8:09 *linkages if and only if all bar lengths remain fixed* (3.2) *and all vertex-edge sided-*
K8:10 *ness conditions* (3.3)*, all vertex-chain noncrossing conditions* (3.5)*, and all edge-*
K8:11 *edge sidedness conditions* (3.6) *are satisfied, for all points $\mathbf{p} = \mathbf{p}(t)$, $0 \le t \le T$.*
K8:12 *(For the vertex-chain noncrossing conditions* (3.5)*, we must consider the motion*
K8:13 *in the space $\hat{\mathbf{p}}(t) \in \mathbb{R}^{2n+4m}$, for some m, which includes the additional parameters*
K8:14 *$\bar{a}_{ik}, \bar{b}_{ik}, a_{ik}, b_{ik}$.)* □

K8:15 Given that we have not formally defined the configuration space, one could
K8:16 also use this lemma as a *definition* of the configuration space. It provides a local
K8:17 coordinatization and algebraic description of the $r_0/4$-neighborhood of any given
K8:18 configuration, essentially covering the configuration space by balls of constant size
K8:19 in which the structure of the configuration space is explicitly given.

K8:20 The lemma also shows that, locally, the configuration space has the structure
K8:21 of a semi-algebraic set, i.e., a set defined by a Boolean combination of polynomial
K8:22 equations and inequalities.

K8:23 A more local characterization is possible by considering only those constraints
K8:24 that are *active*, i.e., coming from vertices that actually lie *on* an edge or another
K8:25 vertex. A vertex-edge sidedness condition (3.3) is active when $\mathbf{p}_k$ touches the
K8:26 interior of the edge $\mathbf{p}_i\mathbf{p}_j$ but does not coincide with an endpoint $\mathbf{p}_i$ or $\mathbf{p}_j$. (In
K8:27 contrast to Lemma 3.1, we do not care about the distance $\|\mathbf{p}_k - \mathbf{p}_i\|$ or $\|\mathbf{p}_k -$
K8:28 $\mathbf{p}_j\|$ when we define whether the constraint is active.) A vertex-chain noncrossing
K8:29 condition (3.5) is active if $\mathbf{p}_i = \mathbf{p}_k$. Finally, an edge-edge sidedness condition (3.6)
K8:30 is active if $\mathbf{p}_i = \mathbf{p}_l$ *and* the two edges $\mathbf{p}_i\mathbf{p}_j$ and $\mathbf{p}_l\mathbf{p}_k$ are parallel and point in the
K8:31 same direction. An inactive constraint does not restrict a motion that is so small
K8:32 that the constraint cannot possibly become active. This threshold is determined by
K8:33 the minimum nonzero distance r_1 between two vertices or between a vertex and an
K8:34 edge, in a given configuration. Unlike r_0, this quantity may depend on the given
K8:35 configuration. We have the following direct corollary of Lemma 3.1.

K8:36 LEMMA 3.2. *Let r_1 be the minimum positive distance between two vertices or*
K8:37 *between a vertex and an edge in a given self-touching configuration. with coordinate*
K8:38 *vector $\mathbf{p}^*$. Consider a path $\mathbf{p}(t) \in \mathbb{R}^{2n}$, $0 \le t \le T$ and with $\mathbf{p}(0) = \mathbf{p}^*$, within the*
K8:39 *$r_1/2$-neighborhood of $\mathbf{p}^*$. This path represents a feasible motion in the configuration*
K8:40 *space of self-touching linkages if and only if all bar lengths remain fixed and all active*
K8:41 *conditions* (3.3)*,* (3.5)*, and* (3.6) *are satisfied for all points $\mathbf{p} = \mathbf{p}(t)$, $0 \le t \le T$.* □

K8:42 The set of constraints in the lemma can be simplified for practical purposes, by
K8:43 looking at the combination of several conditions which restrict the relative motion
K8:44 of two vertices. We will make a few of these simplifications later in Section 6 when
K8:45 we consider the infinitesimal motions of a given configuration.

4. Locked Linkages

Locked configurations. There are two basic notions of being "locked"; the first notion is the most commonly defined in previous work, but the second notion better captures the intended essence of previous examples. (1) We call a self-touching linkage *locked* or *stuck* if the configuration space has multiple connected components within the class of embeddings with the same combinatorial planar embedding. (2) We call a self-touching configuration *locked within* ε if no path in the configuration space (motion) can get outside of a surrounding ball of radius ε. The second definition is stronger for sufficiently small ε, provided that there are other configurations which represent the same combinatorial embedding.

Rigid configurations. One instance of the second definition is the following: a self-touching configuration is called *rigid* if it is locked within 0, that is, there is no motion to a distinct self-touching configuration. This notion is not useful for simple configurations of arcs, cycles, and trees, which are always *flexible* (not rigid). One key feature of self-touching configurations of such linkages is that they can be rigid; other examples of rigid configurations that arise throughout rigidity theory are linkages that form a complex graph structure (consisting of multiple cycles).

Perturbations. To introduce a stronger notion of being locked, we give the following definition. A *δ-perturbation* of a self-touching configuration is a repositioning of the vertices within disks of radius δ that remains consistent with the combinatorial description defined in Section 2. More precisely, for $\delta < r_1/2$, a δ-perturbation must satisfy all active constraints given in Lemma 3.2. A key aspect of a perturbation is that it allows the bar lengths to change slightly (each by at most 2δ).

Conjecture 4.1. *For every self-touching configuration and for every $\delta > 0$, there is a δ-perturbation that is a simple configuration.*

From the definition we can easily obtain a representation where every edge is represented by a polygonal arc, but it seems difficult to simultaneously straighten these arcs.

Strongly locked configurations. Now, a self-touching configuration is *strongly locked* if, for every $\varepsilon > 0$, there is a $\delta > 0$ such that every δ-perturbation is locked within ε. In particular, all sufficiently small simple perturbations are locked. Thus, assuming Conjecture 4.1, the definition of strongly locked configurations provides a connection between the less-intuitive notion of self-touching configurations and the more commonly studied notion of simple configurations. Typically, in particular for the examples considered here, the self-touching configuration arises naturally from a simple configuration, so we need not rely on Conjecture 4.1.

Our goal is to connect strongly locked configurations to notions in rigidity theory which are described in the next section.

5. Rigidity Background

The notions of rigidity, infinitesimal rigidity, and equilibrium stresses are well-understood for *bar frameworks*, configurations of linkages whose bars are permitted to cross each other, and even *tensegrity frameworks* which contain struts and cables that can change their length only monotonically; see [**CDR02, AR78, AR79, Con80, Con82, Con93, CW96, CW93, CW82, CW94, GSS93, RW81, Whi84a, Whi84b, Whi87, Whi88, Whi92**]. This section gives a brief summary

of the relevant material, so that we can generalize it to self-touching configurations of linkages whose bars cannot cross.

Rigidity. A *motion* of a tensegrity framework $\mathbf{p}$ is a continuous function $\mathbf{p}(t)$, $0 \le t \le T$ for some $T > 0$, with $\mathbf{p}(0) = \mathbf{p}$, that preserves the bar lengths according to equation (3.2). A motion is *trivial* if it is a rigid motion (translation and/or rotation). A tensegrity framework $\mathbf{p}$ is *rigid* if it has no nontrivial motion. This definition is a variation of the definition of rigidity for self-touching linkages given in the previous section.

Infinitesimal rigidity. A tensegrity framework is *infinitesimally rigid* if it has no nontrivial infinitesimal motion. An *infinitesimal motion* is an assignment of velocity vectors $\mathbf{v}_i$ to vertices $\mathbf{p}_i$ that preserves bar lengths to the first order:

$$(\mathbf{p}_i - \mathbf{p}_j) \cdot (\mathbf{v}_i - \mathbf{v}_j) = 0 \quad \text{for every bar } \{i, j\}. \tag{5.1}$$

Not every infinitesimal motion can be extended to a motion. Thus, rigidity does not imply infinitesimal rigidity, but the converse implication holds, since a suitable motion can be converted into an infinitesimal motion by taking the derivative at time 0:

LEMMA 5.1. [**CW96, RW81**] *If a tensegrity framework is infinitesimally rigid, then it is rigid.*

We will generalize this result to self-touching linkages in the next section.

Struts. In addition to bars, a framework may have some edges marked as *struts*. The definitions above change as follows in the presence of struts. A motion can never decrease the length of a strut, but may now increase the length of a strut. An infinitesimal motion cannot decrease the length of a strut to the first order:

$$(\mathbf{p}_i - \mathbf{p}_j) \cdot (\mathbf{v}_i - \mathbf{v}_j) \ge 0 \quad \text{for every strut } \{i, j\}. \tag{5.2}$$

In addition to struts, tensegrity frameworks may also contain *cables*, whose change of length is restricted in the opposite direction. We will not use cables in this paper. Lemma 5.1 holds in the presence of struts and cables as well.

Equilibrium stress. A classic duality result connects infinitesimally rigidity to "equilibrium stresses." A *stress* ω assigns a real number $\omega_{\{i,j\}}$ to each bar $\{i, j\}$ and a nonpositive real number $\omega_{\{i,j\}} \le 0$ to each strut $\{i, j\}$. Intuitively, if the stress is negative, then the bar or strut pushes against its endpoints by a force proportional to the stress; and if the stress is positive, then the bar pulls on the two ends by the same amount. A stress is *in equilibrium* if these forces add up to zero:

$$\sum_j \omega_{\{i,j\}}(\mathbf{p}_j - \mathbf{p}_i) = 0, \quad \text{for every vertex } i. \tag{5.3}$$

Infinitesimal rigidity is closely related to equilibrium stress:

LEMMA 5.2. [**RW81**] *If a tensegrity framework is infinitesimally rigid, then it has an equilibrium stress that is nonzero on all struts and cables.*

The converse of this lemma holds under an additional assumption:

LEMMA 5.3. [**RW81**, Theorem 5.2] *If a tensegrity framework has an equilibrium stress that is nonzero on all cables and struts, and the framework becomes infinitesimally rigid when each strut and cable is replaced by a bar, then the original framework is infinitesimally rigid.*

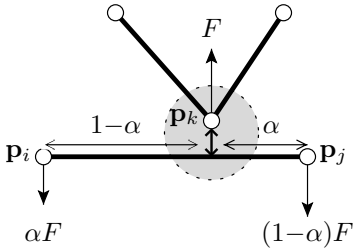

FIGURE 6. Sliding zero-length strut (small double arrow) and proportional distribution of stress F (single arrows). Bold edges denote bars.

K11:01 K11:02 K11:03 K11:04 K11:05 K11:06 K11:07 *Connection to linear programming.* A useful feature of infinitesimal motions is that the bar constraints (5.1) and strut constraints (5.2) are linear equations and inequalities, where $\mathbf{p}$ is known and $\mathbf{v}$ is unknown, and hence can be solved via linear programming. If the linear program can be solved only by trivial (rigid) motions, then the configuration is infinitesimally rigid, and the dual linear program provides an equilibrium stress. (The stresses ω are precisely the dual variables.) This connection to linear programming is a property we will strive for in our setting.

K11:08 ## 6. Infinitesimal Motions for Self-Touching Linkages

K11:09 K11:10 K11:11 K11:12 K11:13 K11:14 K11:15 For simple configurations of linkages whose bars are not permitted to cross, the noncrossing constraint automatically holds for a sufficiently short interval of time, so the notions of rigidity and infinitesimal rigidity remain unchanged. For self-touching configurations, however, the noncrossing constraint introduces additional restrictions at the very beginning of motion. Indeed, this property is the key advantage of self-touching configurations, and is what brings locked configurations into the realm of rigidity theory.

K11:16 K11:17 K11:18 K11:19 K11:20 K11:21 K11:22 The generalizations of motions and thus rigidity is straightforward: motions correspond to paths in the configuration space which has the additional restrictions described in Section 3. For infinitesimal motions, we need to determine the first-order noncrossing constraints. We will look at the active constraints specified in Lemma 3.2 and translate them into constraints on the velocities $\mathbf{v}_i$. They will turn out to be polyhedral (piecewise linear) constraints, but unfortunately, they are not always convex.

K11:23 ### 6.1. Vertices lying on an edge.

K11:24 K11:25 K11:26 K11:27 K11:28 K11:29 *Sidedness constraint.* The simplest type of constraint arises when a vertex $\mathbf{p}_k$ hits the relative interior of a bar $\mathbf{p}_i\mathbf{p}_j$, but not one of the bar's endpoints $\mathbf{p}_i$ or $\mathbf{p}_j$. See Figure 6. In the combinatorial description defined in Section 2, this situation arises when there is a terminal-terminal connection in the magnified view. This situation causes a vertex-edge sidedness constraint (3.3) which we have denoted by $L(i, j; k)$: $\mathbf{p}_k$ must remain on the left side of the line through $\mathbf{p}_i$ and $\mathbf{p}_j$.

K11:30
$$\text{area}(\triangle \mathbf{p}_i(t), \mathbf{p}_j(t), \mathbf{p}_k(t)) \geq 0. \tag{6.1}$$

K11:31 K11:32 For infinitesimal motions, we take the derivative at time $t = 0$, noting that the expression is initially zero, and we get the following necessary condition:

K11:33
$$(\mathbf{p}_i - \mathbf{p}_j)^\perp \cdot \mathbf{v}_k + (\mathbf{p}_j - \mathbf{p}_k)^\perp \cdot \mathbf{v}_i + (\mathbf{p}_k - \mathbf{p}_i)^\perp \cdot \mathbf{v}_j \geq 0, \tag{6.2}$$

where $\binom{x}{y}^{\perp} = \binom{-y}{x}$ denotes a counterclockwise rotation by 90°.

Because the three vectors $(\mathbf{p}_j - \mathbf{p}_i)^{\perp}$, $(\mathbf{p}_i - \mathbf{p}_k)^{\perp}$, and $(\mathbf{p}_k - \mathbf{p}_j)^{\perp}$ are parallel, we can also denote this constraint differently, using the representation of $\mathbf{p}_k$ as a convex combination of $\mathbf{p}_i$ and $\mathbf{p}_j$, $\mathbf{p}_k = \alpha\mathbf{p}_i + (1-\alpha)\mathbf{p}_j$ with $0 < \alpha < 1$:

$$\mathbf{v}_k \cdot \mathbf{b} \geq (1-\alpha)\mathbf{v}_i \cdot \mathbf{b} + \alpha\mathbf{v}_j \cdot \mathbf{b} \quad \text{where } \mathbf{b} = (\mathbf{p}_j - \mathbf{p}_i)^{\perp} \tag{6.3}$$

We denote this constraint by $L'(i,j;k)$ and regard it as a linear inequality in the unknowns $\mathbf{v}$. The notation L' reminds us that it was obtained as a "derivative" of the constraint $L(i,j;k)$.

6.2. Coincident vertices. Consider two vertices i and k that coincide geometrically; refer to Figure 3. We begin by considering the constraints on k, and later return to the constraints on i. As discussed in Section 3.2, vertex k lies in a wedge between two consecutive edges around vertex i. Call the edges $\{j,i\}$ and $\{i,l\}$, so that vertex k lies in the counterclockwise wedge j,i,l. Let φ denote the angle of the wedge. As a special case, vertex i may be incident to only one edge, in which case the two edges bounding the wedge are the same, i.e., $j = l$, and $\varphi = 360°$.

By the vertex-chain noncrossing condition (3.5), the relative first-order movement $\mathbf{v}_k - \mathbf{v}_i$ of $\mathbf{p}_k$ with respect to $\mathbf{p}_i$, is restricted to the angular wedge between the two edges $\mathbf{p}_i\mathbf{p}_j$ and $\mathbf{p}_l\mathbf{p}_i$. For $\varphi \leq 180°$, we have a convex cone, which is described by the conjunction that $\mathbf{p}_k$ must remain to the left of the line $\mathbf{p}_i\mathbf{p}_j$ *and* to the left of the line $\mathbf{p}_l\mathbf{p}_i$ (Figure 3(a)):

$$L'(i,j;k) \wedge L'(l,i;k).$$

For a reflex angle $\varphi > 180°$, we have a nonconvex cone which is described by the disjunction that $\mathbf{p}_k$ must remain to the left of the line $\mathbf{p}_i\mathbf{p}_j$ *or* to the left of the line $\mathbf{p}_l\mathbf{p}_i$ (Figure 3b). We introduce a special notation for this condition

$$M'(i,j,l;k) \iff L'(i,j;k) \vee L'(l,i;k).$$

Note that it is not necessary to introduce the additional parameters $\bar{a}, \bar{b}, a, b$; we can remain in the original space $\mathbb{R}^{2n}$.

The vertex j is restricted by a wedge defined by two consecutive edges around k in the same way, giving rise to further conditions of the above form.

The infinitesimal versions of the edge-edge sidedness conditions (3.6) can be derived in the same way, giving rise to the single linear constraint $L'(i,j;l)$; see Figure 7(c). (The remaining conditions of (3.6) follow from the vertex-edge sidedness constraints.)

There is one case where the above constraints do not describe the local feasible directions of motion completely: If $\varphi = 0$ in the situation of Figure 3, the condition $L'(i,j;k) \wedge L'(l,i;k)$ only constrains $\mathbf{p}_k$ to move on the *line* $\mathbf{p}_i\mathbf{p}_j\mathbf{p}_l$, whereas it must really remain on the *ray* $\mathbf{p}_i\mathbf{p}_j$. In order to remedy this situation and prevent $\mathbf{p}_k$ from "escaping" through $\mathbf{p}_i$ to the opposite side, we could just add another linear constraint "perpendicular" to the constraints $L'(i,j;k)$ and $L'(l,i;k)$. This would then lead to a slightly weaker concept of infinitesimal rigidity in the next subsection. However, to make the theory coherent, we would later (in Section 7) also have to introduce a special kind of strut corresponding to the new constraint, and therefore we leave this extension as an exercise for the reader. The validity of the theorems is not affected by this omission, since the conditions that we have

derived for infinitesimal motions are only *necessary* conditions anyway. In other words, while the definition of infinitesimal motions used in this paper allows a few motions that should not be considered "proper," this makes the notion of infinitesimal rigidity only (slightly) stronger.

6.3. Infinitesimal rigidity. For the feasible directions of motion, we have given a set $\mathcal{M}$ of necessary constraints of the form $L'(i,j;k)$ and $M'(i,j,l;k)$. For such a set $\mathcal{M}$ of constraints, we denote by $P_{\mathcal{M}}$ the set of infinitesimal motions $\mathbf{v}$ that satisfy those constraints and the length preservation equations (5.1). This set is a polyhedral cone. The linkage $\mathbf{p}$ is *infinitesimally rigid* if $P_{\mathcal{M}}$ contains only trivial infinitesimal motions. We have the following generalization of Lemma 5.1:

LEMMA 6.1. *If a self-touching configuration is infinitesimally rigid, then it is rigid.*

PROOF. The proof can be given along the lines of a proof used in the context of "second-order rigidity" [**CW96**, Theorem 4.3.1] to show that second-order rigidity implies rigidity. We only sketch the main idea of the proof here. In a neighborhood of a self-touching configuration $\mathbf{p}$, a motion is confined within a semi-algebraic set defined by the equations and inequalities given in Lemma 3.1. Any point in a semi-algebraic set has a neighborhood with an analytic parameterization; see e.g. [**Mil68**]. Thus, if $\mathbf{p}$ is not rigid, we obtain a short analytic motion $\mathbf{p}(t)$ with $\mathbf{p}(0) = \mathbf{p}$. The tangent direction $\mathbf{v}$ at $\mathbf{p}$ (the first nonvanishing coefficient of the power-series expansion of $\mathbf{p}(t)$ at $t = 0$) is then an infinitesimal motion of $\mathbf{p}$. □

6.4. Reduction to convex cones. Unfortunately, because of the nonconvex constraints $M'(i,j,l;k)$, $P_{\mathcal{M}}$ is in general not convex. In showing that $P_{\mathcal{M}}$ contains only rigid motions (and thus the framework is infinitesimally rigid), we would like to apply linear programming and the duality theory of convex cones.

There are two options to reduce the problem to convex cones. First, we may take the *convex relaxation* by simply ignoring all disjunctive constraints of the form $M'(i,j,l;k)$:

$$P_{\mathcal{M}} \subseteq P_{\mathcal{M}'},$$

where $\mathcal{M}' \subseteq \mathcal{M}$ contains only the constraints of the form $L'(i,j;k)$. If we succeed in showing that this relaxed cone $P_{\mathcal{M}'}$ contains only the rigid motions, then so does the original cone and we are done.

Second, we can represent the cone as a union of convex cones, by picking one L inequality from each disjunction M of inequalities, and trying all possible combinations. If we have s disjunctions, we obtain 2^s convex cones:

$$P_{\mathcal{M}} = P_{\mathcal{M}_1} \cup P_{\mathcal{M}_2} \cup P_{\mathcal{M}_3} \cup \cdots \cup P_{\mathcal{M}_{2^s}}$$

Each of these cones is convex, so we can check the existence of nontrivial solutions in each of these cones by linear programming or by the techniques discussed in Section 7.

We summarize the two approaches in a small lemma. We let $G_{\mathcal{M}}$ denote the tensegrity framework corresponding to the set of constraints $\mathcal{M}$.

LEMMA 6.2. (1) *If $G_{\mathcal{M}'}(\mathbf{p})$ is infinitesimally rigid, then so is $G_{\mathcal{M}}(\mathbf{p})$.*

(2) *$G_{\mathcal{M}}(\mathbf{p})$ is infinitesimally rigid if and only if all frameworks $G_{\mathcal{M}_1}(\mathbf{p}), \ldots, G_{\mathcal{M}_{2^s}}(\mathbf{p})$ are infinitesimally rigid.* □

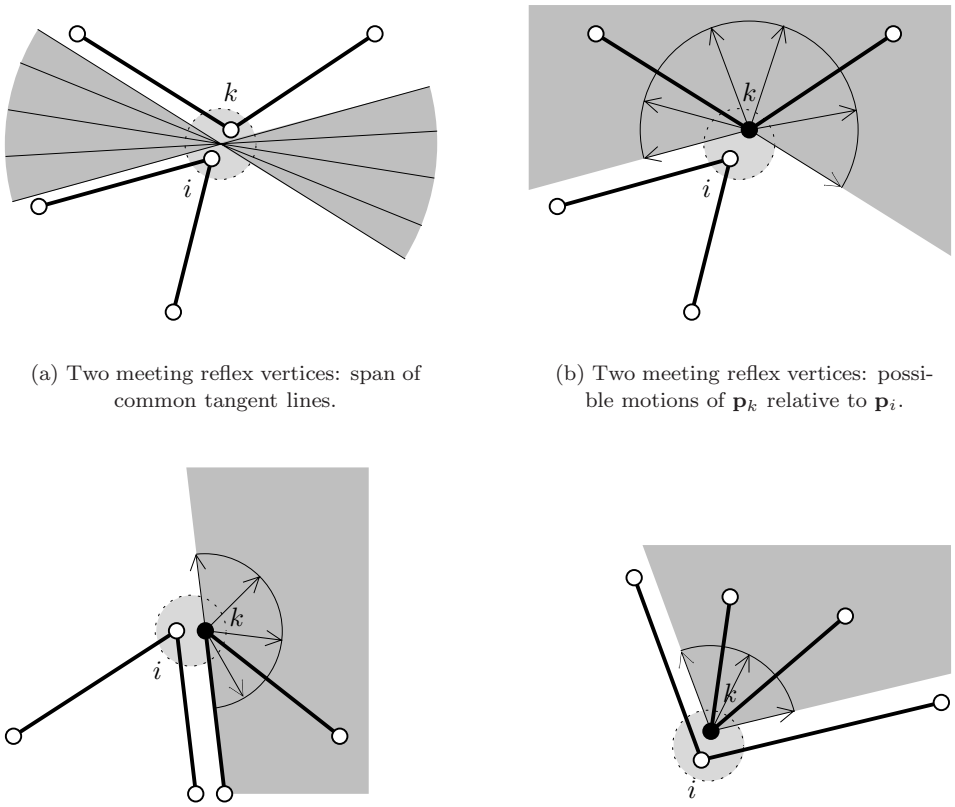

(a) Two meeting reflex vertices: span of common tangent lines.

(b) Two meeting reflex vertices: possible motions of $\mathbf{p}_k$ relative to $\mathbf{p}_i$.

(c) Two meeting reflex vertices sharing an edge direction.

(d) A convex vertex meeting a reflex vertex.

FIGURE 7. Cases of constraint interplay between touching vertices $\mathbf{p}_i$ and $\mathbf{p}_k$. The shaded area in (b), (c), and (d) indicates the range of possible motions of $\mathbf{p}_k$ relative to $\mathbf{p}_i$.

K14:01 Any combination of the two approaches, like in a branch-and-bound tree, is
K14:02 also possible.

K14:03 In some instances, like in Figure 1(a), we do not have a vertex in a reflex
K14:04 wedge as in Figure 3b, and $P_{\mathcal{M}}$ is already a convex cone. But even in other cases,
K14:05 some simplifications are possible. If we look at two coincident vertices j and k,
K14:06 we can combine j's constraints and k's constraints, and instead of two disjunctions
K14:07 of the form $M'(i, j, l; k)$ we get only one disjunction of two linear inequalities, or
K14:08 even convex constraints, as follows. When the two relevant angles at $\mathbf{p}_i$ and $\mathbf{p}_k$
K14:09 are both reflex, the direction of movement $\mathbf{v}_k - \mathbf{v}_i$ is constrained by two extreme
K14:10 directions which correspond to the two extreme directions of a line separating the
K14:11 two chains through $\mathbf{p}_i$ and $\mathbf{p}_k$ locally (Figures 7(a) and 7(b)). This constraint
K14:12 can be represented as a logical disjunction of two linear constraints of the form
K14:13 $L'(i, j; k)$, but not necessarily in the pattern given by $M'(i, j, l; k)$ above. There is
K14:14 one special case when two reflex angles meet but they nevertheless produce a single

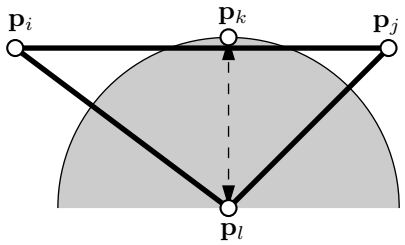

FIGURE 8. A construction replacing a sliding zero-length strut

K15:01 inequality: when the two chains have two edges pointing in the same direction
K15:02 (Figure 7(c)). This is in fact just the infinitesimal version of the edge-edge sidedness
K15:03 conditions (3.6). Finally, when one chain lies inside a convex angle of the other
K15:04 chain, we get a convex wedge which is representable as a conjunction of two linear
K15:05 constraints (Figure 7(d)).

K15:06 It suffices to constrain only those pairs of touching vertices that are combi-
K15:07 natorially adjacent, that is, not obscured from each other by connections in the
K15:08 magnified view. This also eliminates a number of nonconvex constraints.

K15:09 7. Stresses for Self-Touching Linkages

K15:10 In this section we assume that we have no constraints of the form $M'(i,j,l;k)$,
K15:11 and discuss how the sidedness constraints $L'(i,j;k)$ can be treated in using the
K15:12 notion of stresses.

K15:13 *Sliding zero-length struts.* The constraint $L'(i,j;k)$ can be viewed as a *sliding*
K15:14 *zero-length strut* with one end at $\mathbf{p}_k$ and the other end sliding along the bar $\mathbf{p}_i\mathbf{p}_j$
K15:15 to match the orthogonal projection of $\mathbf{p}_k$ onto the bar.

K15:16 *Modeling by tensegrity frameworks.* We can also model these conditions by an
K15:17 auxiliary vertex $\mathbf{p}_l$ and a "classic" strut; see Figure 8. Choose a point $\mathbf{p}_l$ on the line
K15:18 through $\mathbf{p}_k$ perpendicular to $\mathbf{p}_i\mathbf{p}_j$, on the opposite side of where $\mathbf{p}_k$ is constrained
K15:19 to lie. Connect $\mathbf{p}_l$ to $\mathbf{p}_k$ by a strut and to $\mathbf{p}_i$ and $\mathbf{p}_j$ by bars. Then keeping $\mathbf{p}_i$ and
K15:20 $\mathbf{p}_j$ fixed, the point $\mathbf{p}_k$ is prevented from entering the circle around $\mathbf{p}_l$ through $\mathbf{p}_k$.
K15:21 This condition is (locally) weaker than the original sidedness constraint $L'(i,j;k)$.
K15:22 In terms of directions (infinitesimal motions), however, it is equivalent. Thus we
K15:23 have the following statement:

K15:24 LEMMA 7.1. (1) *The augmented bar-and-strut framework is infinitesimally rigid*
K15:25 *if and only if the original self-touching linkage is infinitesimally rigid.*
K15:26 (2) *If the augmented bar-and-strut framework is rigid then the original self-*
K15:27 *touching linkage is rigid.* □

K15:28 We do not know whether equivalence holds for rigidity, too.

K15:29 *Stress.* The proper generalization of stresses for frameworks with sidedness con-
K15:30 straints may be derived in two ways. First, they are the dual variables corresponding
K15:31 to the infinitesimal sidedness constraints $L'(i,j;k)$; secondly, we may consult the
K15:32 stress in the augmented framework with the auxiliary network. Both approaches
K15:33 lead to the same intuitive result, as shown in Figure 6. A stress of $F = \omega_{k,ij} \leq 0$
K15:34 on a sliding strut induces a force of magnitude $-F$ on $\mathbf{p}_k$ perpendicular and to the
K15:35 left of bar $\mathbf{p}_i\mathbf{p}_j$, and the opposite force is distributed proportionally to $\mathbf{p}_i$ and $\mathbf{p}_j$

based on their relative proximity to $\mathbf{p}_k$. More precisely, $\mathbf{p}_i$ feels a force of $-\alpha F$ perpendicular and to the right of bar $\mathbf{p}_i\mathbf{p}_j$, and $\mathbf{p}_j$ feels a force of $-(1-\alpha)F$ perpendicular to the right of bar $\mathbf{p}_i\mathbf{p}_j$. In an equilibrium stress, the sum of these forces at each vertex must leave the vertex stationary as in (5.3).

Connections between infinitesimal rigidity and equilibrium stress. Lemmas 5.2 and 5.3 can be directly applied to the tensegrity frameworks derived above with the auxiliary vertices. They can also be translated into the notions of sliding zero-length struts. We need to define a *sliding zero-length bar*: such a bar restricts $\mathbf{p}_k$ to remain on (the left side of) the bar $\mathbf{p}_i\mathbf{p}_j$, but leaves $\mathbf{p}_k$ free to slide along the bar.

LEMMA 7.2. *A self-touching configuration is infinitesimally rigid if and only if the following two conditions hold*:

(1) *the configuration becomes infinitesimally rigid when each sliding zero-length strut is replaced by a sliding zero-length bar, and*
(2) *the self-touching framework has a stress that is negative on every sliding zero-length strut.* □

8. Connection Between Rigid and Locked

The relevance of the generalized rigidity theory developed in the previous section is the following connection between rigid and locked linkages:

THEOREM 8.1. *If a self-touching configuration is rigid, then it is strongly locked.*

In fact, we will show this result even when the δ-perturbations are permitted to satisfy the bar and noncrossing constraints approximately, up to tolerance 2δ. This result is an extension of a result about "sloppy rigidity" [**Con82**, Theorem 1] stating essentially the same result (in different words) for tensegrity frameworks. Our proof follows the same outline. A different proof, working on the stronger assumption of *infinitesimal* rigidity, is given in the appendix. That proof, however, has the advantage of providing explicit bounds on δ in terms of ε.

PROOF. The proof is based on a topological argument about closed sets of configurations and their neighborhoods.

LEMMA 8.2. *Let $A_\delta \subseteq \mathbb{R}^m$ $(\delta \geq 0)$ be a family of closed sets with $A_\delta \subseteq A_{\delta'}$ for $0 \leq \delta < \delta'$ and*

$$\bigcap_{\delta>0} A_\delta = A_0.$$

For $\mathbf{p} \in A_\delta$ we denote by $B_\delta(\mathbf{p})$ the set of points which are reachable by a curve in A_δ starting at $\mathbf{p}$. Let $\mathbf{p}^* \in A_0$, suppose that the set $B_0 := B_0(\mathbf{p}^*)$ is compact, and there is a positive lower bound on the distance between B_0 and any point in $A_0 - B_0$.

Then for every $\varepsilon > 0$ there exists a $\delta > 0$ with the following property: $\|\mathbf{p}-\mathbf{p}^*\| < \delta$ implies that $B_\delta(\mathbf{p})$ is contained in an ε-neighborhood of B_0.

The last statement simply means that $d_{\min}(\mathbf{q}, B_0) \leq \varepsilon$ for all $\mathbf{q} \in B_\delta(\mathbf{p})$, where $d_{\min}(\mathbf{q}, X)$ denotes the distance from $\mathbf{q}$ to the closest point in the set X.

The easy proof of the lemma is given at the end. Let $\mathbf{p}^*$ be a rigid self-touching configuration. We apply the lemma to the sets A_δ of configurations $\mathbf{p}$ that are

defined by relaxing the length constraints for the bars:

$$\|\mathbf{p}_i^* - \mathbf{p}_j^*\| - 2\delta \;\le\; \|\mathbf{p}_i - \mathbf{p}_j\| \;\le\; \|\mathbf{p}_i^* - \mathbf{p}_j^*\| + 2\delta \quad \text{for every bar } \{i,j\}. \tag{8.1}$$

In addition, $\mathbf{p}$ must satisfy the sidedness and noncrossing conditions of Lemma 3.1. Then the set A_δ, viewed as a subset of the enlarged space $\mathbb{R}^{2n+4m}$ (with all of the parameters $\bar{a}, \bar{b}, a, b$ from (3.5)) contains all δ-perturbations $\mathbf{p}$ of $\mathbf{p}^*$. By Lemma 3.1, the sidedness and noncrossing constraints are valid as long as $\mathbf{p}$ does not deviate by more than $r_0/2$ from $\mathbf{p}^*$.

The assumption that $\mathbf{p}^*$ is rigid means that B_0 contains precisely the configurations that are rigid motions of $\mathbf{p}^*$. To achieve compactness of B_0 we fix the position of one vertex. This can be done without changing the problem. The set A_0, being a semi-algebraic set, is locally arcwise connected, and therefore B_0 is the component of A_0 containing $\mathbf{p}^*$, and there is a positive lower bound on the distance between B_0 and $A_0 - B_0$. Thus, the assumptions of the lemma are fulfilled.

The set $B_\delta(\mathbf{p})$ contains those configurations that are reachable by a weakly simple motion from $\mathbf{p}$. The allowed curves in $B_\delta(\mathbf{p})$ are even more relaxed, because the bar lengths $\|\mathbf{p}_i - \mathbf{p}_j\|$ can vary freely within the interval $\|\mathbf{p}_i^* - \mathbf{p}_j^*\| \pm 2\delta$ during the "motion".

If we start a motion in any δ-perturbation $\mathbf{p}$ of $\mathbf{p}^*$, we must remain inside $B_\delta(\mathbf{p})$, as long as $d_{\min}(\mathbf{p}, B_0) < r_0/2$. Let us choose any ε with $0 < \varepsilon < r_0/2$. Then the lemma implies that a $\delta > 0$ exists such that starting in $\mathbf{p}$ with $\|\mathbf{p} - \mathbf{p}^*\| < \delta$ we must always remain ε-close to $\mathbf{p}^*$, up to some rigid motion. This means that $G(\mathbf{p}^*)$ is strongly locked. □

Proof of the lemma. We prove the lemma by contradiction. Let $\varepsilon_1 > 0$ be a number smaller than the minimum distance between B_0 and $A_0 - B_0$. Suppose to the contrary that, for some fixed ε with $0 < \varepsilon < \varepsilon_1$ and for all δ with $0 < \delta < \varepsilon$, there is a point $\mathbf{p}$ with $\|\mathbf{p} - \mathbf{p}^*\| < \delta$ and a point $\bar{\mathbf{q}} \in B_\delta(\mathbf{p})$ with $d_{\min}(\bar{\mathbf{q}}, B_0) > \varepsilon$. We denote by $H^<$, $H^=$, and $H^>$ the set of points x for which $d_{\min}(x, B_0)$ is less than, equal to, or bigger than ε. We have $\bar{\mathbf{q}} \in H^>$, and because $d_{\min}(\mathbf{p}, B_0) \le \|\mathbf{p} - \mathbf{p}^*\| \le \delta < \varepsilon$, we have $\mathbf{p} \in H^<$. Because $\mathbf{p}$ and $\bar{\mathbf{q}}$ are connected in $B_\delta(\mathbf{p})$ we can find another point $\mathbf{q} \in B_\delta(\mathbf{p}) \cap H^=$,

Consider an infinite sequence $\delta_1, \delta_2, \ldots$ with $0 < \delta_i < \varepsilon$ converging to 0, and consider the corresponding sequence of points $\mathbf{p}_i$ and $\mathbf{q}_i$ with $\|\mathbf{p}_i - \mathbf{p}^*\| < \delta_i$, $\mathbf{q}_i \in B_{\delta_i}(\mathbf{p}_i) \subseteq A_{\delta_i}$, and $\mathbf{q}_i \in H^=$. Because the $\mathbf{q}_i$ lie in the compact set $H^=$, there is an infinite subsequence converging to a limit configuration $\mathbf{q}^* \in A_0 \cap H^=$, a contradiction. □

9. Proving a Linkage to be Strongly Locked

Using the tools above, we can follow the following outline for proving that a particular linkage is strongly locked:

1. Model the linkage as a small perturbation of a self-touching linkage with slightly different edge lengths.
2. Check that the self-touching linkage is infinitesimally rigid. When the constraints are convex, or using the techniques in Section 6.4, this can be done by linear programming.
3. If the answer to the second step is "yes," then the self-touching linkage is strongly locked, and hence sufficiently close perturbations of the original linkage are locked within an arbitrarily small ε.

K18:01 The key advantage of this approach is that all but the first step is algorithmic.
K18:02 We also find that the first step typically matches the intuition of previously proposed
K18:03 examples and hence applies; the examples in the next section justify this statement.
K18:04 A limitation of the approach is that the test is conservative: an infinitesimally
K18:05 flexible linkage may still be strongly locked, and even if the self-touching linkage is
K18:06 not strongly locked, the original linkage may still be locked. In particular, the com-
K18:07 plexity of deciding whether a particular linkage is locked remains open. However,
K18:08 we find this conservative test to suffice in many examples, to which we now turn.
K18:09 To make the examples more explicit, we expand the second step into two steps
K18:10 which turn out to be easy to execute by hand, although they are slightly more
K18:11 conservative:

K18:12 (2) Check whether the self-touching linkage is infinitesimally rigid:
K18:13 (a) Check that the bar version of the self-touching linkage is infinitesi-
K18:14 mally rigid.
K18:15 This step is normally quite easy because the sliding zero-length bars
K18:16 restrict motions severely, often creating rigid triangles.
K18:17 (b) Prove that the self-touching linkage has an equilibrium stress that is
K18:18 nonzero on all struts (or verify via linear programming).
K18:19 Such a stress can sometimes be constructed very easily. For exam-
K18:20 ple, one can superimpose stresses on simple structures like complete
K18:21 graphs on four vertices, where the stress is unique up to a scalar
K18:22 multiple. Or one can construct the stress incrementally: at a ver-
K18:23 tex of degree 3, the stress is unique up to a scalar multiple. One
K18:24 can start at such a vertex and establish equilibrium as one proceeds
K18:25 through a sequence of vertices. In the examples below, this procedure
K18:26 can be carried out without any computational effort, by just paying
K18:27 attention to the sign pattern.

K18:28 If both parts succeed, then by Lemma 7.2 the self-touching linkage is infinitesimally
K18:29 rigid, and hence by Theorem 8.1 it is strongly locked.
K18:30 Along the way, we may need to deal with touching vertices as described in
K18:31 Section 6.4.

K18:32 ## 10. Locked Trees

K18:33 ### 10.1. Original tree.

K18:34 *Step 1*: *Model as a self-touching linkage.* Our approach applies directly to the
K18:35 pinwheel tree in Figure 1(a), or more precisely the self-touching version of the tree,
K18:36 because the ends of the arms touch the center vertex in a convex angle, and those
K18:37 are the only touching pairs of vertices. We focus on one sector of the pinwheel, as
K18:38 shown in Figure 9, and extend the stress to the whole tree by symmetry.
K18:39 *Step 2a*: *Bar version is infinitesimally rigid.* In the bar version of the self-
K18:40 touching tree, C is constrained to slide along both OA and OA'', and hence C
K18:41 is pinned against O. The velocity vector $\mathbf{v}_C$ must be parallel to both OA and
K18:42 OA'', and hence must be 0. Thus $OABC$ forms a rigid triangle. We get eight
K18:43 rigid triangles which are connected at the common vertex O. Because B can only
K18:44 slide along OA'', the triangle OAB is effectively glued to the next triangle $OA''B''$,
K18:45 with whom it shares the vertex O. So all triangles are glued together in a cyclic
K18:46 sequence, and the bar version is infinitesimally rigid.

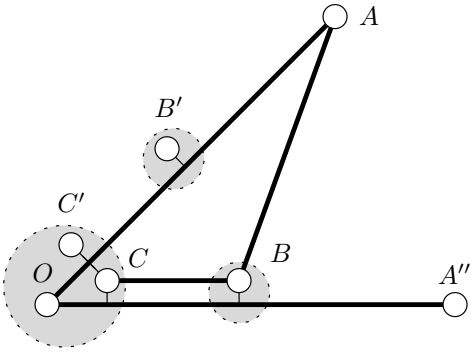

FIGURE 9. One sector of the self-touching tree from Figure 1(a). The vertices of focus form the chain $OABC$; also shown are the analog A'' of A for the clockwise adjacent wedge, and the analogs B', C' of B and C for the counterclockwise adjacent wedge. Thick edges denote bars, and thin edges denote sliding zero-length struts.

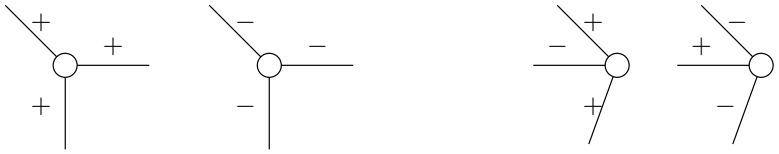

(a) 3 incident edges not in a halfplane. (b) 3 incident edges in a halfplane.

FIGURE 10. Possible sign patterns for an equilibrium stress at a degree-3 vertex when no two of the edges are collinear.

K19:01 *Step 2b*: *Existence of equilibrium stress.* To construct the stress with the de-
K19:02 sired signs, it is helpful to imagine little springs at the struts and to think how their
K19:03 forces would be transmitted.

K19:04 We construct the stress incrementally: A vertex with three incident stresses (not
K19:05 all parallel) has a unique equilibrium solution for those stresses, up to multiplication
K19:06 by a constant. The possible sign patterns at such a vertex are shown in Figure 10.
K19:07 Vertex C is of type (a), so all three signs are equal. We start by giving the three
K19:08 edges incident to C a negative stress: $\omega_{C,OA} < 0$, $\omega_{C,OA''} < 0$, and $\omega_{CB} < 0$. We
K19:09 balance the force from CB at B by two (uniquely determined) stresses $\omega_{B,OA''} < 0$,
K19:10 and $\omega_{BA} < 0$. We repeat these stresses symmetrically for all sections around the
K19:11 wheel. By symmetry, this will establish equilibrium at O. We now still have
K19:12 unresolved forces at A and the analogous vertices $A', A'', \ldots$. The direction of the
K19:13 force at A must be parallel to OA because otherwise all the forces would generate a
K19:14 nonzero rotational moment around O. This is impossible, because individual forces
K19:15 generated by the stresses ω_{ij} and $\omega_{k,ij}$ are torque-free. Thus the forces at A (and
K19:16 $A', \ldots$) can be canceled by stresses $\omega_{OA} > 0$, without destroying equilibrium at O.
K19:17 This stress is negative on all struts.

K19:18 *Step 3*: *Finale.* By Lemma 7.2, the self-touching linkage is infinitesimally rigid,
K19:19 so by Lemma 6.1 it is also rigid, so by Theorem 8.1 it is also strongly locked. Hence,
K19:20 if the original tree in Figure 1(a) is drawn sufficiently tight, then it is locked within
K19:21 some small ε.

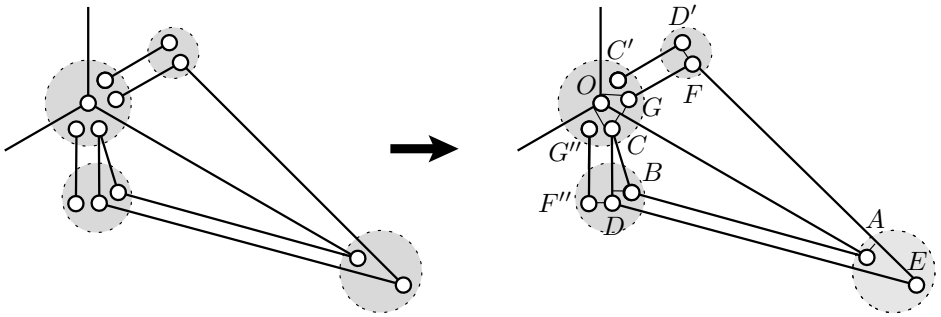

FIGURE 11. One arm of the tree in Figure 1(c). The vertices of focus form the chain $OABCDEFG$; also shown are the analogs F'', G'' of F, G for the clockwise adjacent wedge, and the analogs C', D' of C, D for the counterclockwise adjacent wedge. Thick edges denote bars, and thin edges denote sliding zero-length struts. Only the struts which are used to prove rigidity are shown.

K20:01 K20:02 Given the setup from the previous sections, this proof is simpler than the original proof that this tree is locked [**BDD$^+$02**].

K20:03 **10.2. New tree.**

K20:04 K20:05 K20:06 K20:07 K20:08 *Step 1*: *Model as self-touching linkage.* To apply the approach to the tree in Figure 1(c) in a similarly easy way, we drop some of the struts; see Figure 11. If we can show that the linkage with fewer struts is infinitesimally rigid, the original linkage must also be infinitesimally rigid. Again, we exploit symmetry and focus on one portion of the linkage.

K20:09 K20:10 K20:11 K20:12 K20:13 K20:14 K20:15 K20:16 K20:17 K20:18 *Step 2a*: *Bar version is infinitesimally rigid.* C is constrained to slide along both OA and OA'', and hence C is stuck at O. The same argument holds for G and G''. The sliding struts between B and D, and between D and F'', perpendicular to CD now hold B, D and F'' together. Thus $OABDC$ forms a rigid triangle, with $O = A$ and $B = D$. If we regard this triangle as fixed, the bar DE constrains the infinitesimal motion of E to directions perpendicular to DE, whereas the sliding strut which keeps A on EF restrains the relative motion of A and E to directions parallel to EF. This prevents any relative motion of E with respect to A, making the triangle $OAEFG$ rigid too. So we get a rigid structure of six triangles glued together around O in a cyclic fashion.

K20:19 K20:20 K20:21 K20:22 K20:23 *Step 2b*: *Existence of equilibrium stress.* We will construct a stress which is negative on all struts. For simplicity, we write ω_{BD} for the stress between B and D in the direction perpendicular to OB. This stress can be interpreted as $\omega_{B,CD}$, as suggested by the figure, or as $\omega_{D,BC}$; it does not matter which. Similarly, we will use $\omega_{DF''}$ and $\omega_{D'F}$.

K20:24 K20:25 K20:26 K20:27 K20:28 K20:29 We start with an equilibrium at F by giving the three incident edges a negative stress: $\omega_{FG} < 0$, $\omega_{EF} < 0$, and $\omega_{D'F} < 0$. The negative force at G can be canceled by negative stresses $\omega_{G,OA} < 0$ and $\omega_{G,OA'} < 0$. Now E has two more edges besides EF; we create equilibrium at E by setting $\omega_{A,EF} < 0$ and $\omega_{DE} > 0$. (To see the correct sign pattern, one must draw the sliding strut with stress $\omega_{A,EF} < 0$ attached to E and not to A as in the figure.)

All of this is of course done symmetrically in the three arms of the tree. So the vertex D already has a stress $\omega_{DF''} < 0$ which is determined, in addition to $\omega_{DE} > 0$ which we just fixed. The resulting force induces a unique solution for ω_{BD} and ω_{CD}. We can find this solution in two steps. First we ignore $\omega_{DF''}$ and get an equilibrium with $\omega_{DE} > 0$, $\omega^0_{BD} < 0$, and $\omega_{CD} > 0$. Now $\omega_{DF''} < 0$ can be canceled by further decreasing ω_{BD} to its final value $\omega^1_{BD} < \omega^0_{BD} < 0$. We extend $\omega^1_{BD} < 0$ to an equilibrium at B by setting $\omega_{BC} < 0$ and $\omega_{AB} < 0$. The situation in B is almost the same as in D when we first constructed the equilibrium in B with the initial value ω^0_{BD}: The three edges point in parallel directions and have the same lengths. The difference is that ω_{BD} points in the opposite direction when seen from B, and $|\omega^1_{BD}| > |\omega^0_{BD}|$. It follows for the corresponding parallel edges CD and BC that $|\omega_{BC}| > |\omega_{CD}|$.

Therefore, in C, the negative stress ω_{BC} prevails over the positive stress ω_{CD}, resulting in a negative total force in C from the direction of B and D: $\omega_{BC}+\omega_{CD} < 0$. This force is canceled by negative stresses $\omega_{C,OA} < 0$ and $\omega_{C,OA''} < 0$.

We can now conclude as for the simple tree. By symmetry, O must be in equilibrium, and the three remaining forces in A, A', and A'' must be parallel to OA, OA', and OA'', respectively, so they can be canceled by appropriate stresses on those edges.

Step 3: *Finale.* By Lemma 7.2, the self-touching linkage is infinitesimally rigid, so by Lemma 6.1 it is also rigid, so by Theorem 8.1 it is also strongly locked. Hence, if the original tree in Figure 1(c) is drawn sufficiently tight, then it is locked within an arbitrarily small ε. In the appendix we show that any δ-perturbation of the tree is locked within 0.0001, for $\delta = 3 \times 10^{-8}$.

11. Conclusion

To study when linkages are locked, we developed the notion of a *self-touching* linkage which captures instantaneous crossing constraints. We then generalized rigidity theory to capture such noncrossing constraints, the difficulty being that in some cases the constraints are nonconvex. We proved that rigidity in this setting implies that the linkage is *strongly locked*, meaning that small enough perturbations of the linkage can barely move, as little as desired. In particular, this brings results about self-touching linkages into the commonly studied realm of strictly simple, nontouching linkages.

Our theory can be used to prove a variety of linkages to be strongly locked. In particular, we showed two examples here: the tree from [**BDD+02**], and a new tree with a single degree-3 vertex.

References

[AR78] L. Asimow and B. Roth, *The rigidity of graphs*, Transactions of the American Mathematical Society **245** (1978), 279–289.

[AR79] L. Asimow and B. Roth, *The rigidity of graphs. II*, Journal of Mathematical Analysis and Applications **68** (1979), no. 1, 171–190.

[BDD+02] Therese Biedl, Erik Demaine, Martin Demaine, Sylvain Lazard, Anna Lubiw, Joseph O'Rourke, Steve Robbins, Ileana Streinu, Godfried Toussaint, and Sue Whitesides, *A note on reconfiguring tree linkages*: *Trees can lock*, Discrete Applied Mathematics **117** (2002), 293–297. The full version is Technical Report SOCS-00.7, School of Computer Science, McGill University, September 2000, and Computing Research Repository paper cs.CG/9910024. `http://www.arXiv.org/abs/cs.CG/9910024`.

K22:01 [Can87] John Canny, *A new algebraic method for robot motion planning and real geometry*,
K22:02 Proceedings of the 28th Annual Symposium on Foundations of Computer Science (Los
K22:03 Angeles, California), October 1987, IEEE Computer Society Press, Washington, D.C.,
K22:04 1987, pp. 39–48.
K22:05 [Can88] John Canny, *Some algebraic and geometric computations in PSPACE*, Proceedings of
K22:06 the 20th Annual ACM Symposium on Theory of Computing (Chicago, Illinois), May
K22:07 1988, ACM Press, New York, 1988, pp. 460–469.
K22:08 [CDR02] Robert Connelly, Erik D. Demaine, and Günter Rote, *Straightening polygonal arcs*
K22:09 *and convexifying polygonal cycles*, Discrete & Computational Geometry, to appear.
K22:10 Preliminary version in the Proceedings of the 41st Annual Symposium on Foundations
K22:11 of Computer Science (Redondo Beach, California), November 2000, IEEE Computer
K22:12 Society Press, Washington, D.C., 2000, pp. 432–442; an extended version is available
K22:13 as Technical report B 02-02, Freie Universität Berlin, Institut für Informatik, 2002.
K22:14 [Con80] Robert Connelly, *The rigidity of certain cabled frameworks and the second-order rigid-*
K22:15 *ity of arbitrarily triangulated convex surfaces*, Advances in Mathematics **37** (1980),
K22:16 no. 3, 272–299.
K22:17 [Con82] Robert Connelly, *Rigidity and energy*, Inventiones Mathematicae **66** (1982), no. 1,
K22:18 11–33.
K22:19 [Con93] Robert Connelly, *Rigidity*, in: Handbook of Convex Geometry, vol. A (Peter M. Gruber
K22:20 and Jörg M. Wills, eds.), North-Holland, Amsterdam, 1993, pp. 223–271.
K22:21 [CW82] Henry Crapo and Walter Whiteley, *Statics of frameworks and motions of panel struc-*
K22:22 *tures, a projective geometric introduction (with a French translation)*, Structural
K22:23 Topology **6** (1982), 43–82.
K22:24 [CW93] Henry Crapo and Walter Whiteley, *Autocontraintes planes et polyèdres projetés. I.*
K22:25 *Le motif de base [Plane self stresses and projected polyhedra. I. The basic pattern]*,
K22:26 Structural Topology **20** (1993), 55–78.
K22:27 [CW94] Henry Crapo and Walter Whiteley, *Spaces of stresses, projections and parallel draw-*
K22:28 *ings for spherical polyhedra*, Beiträge zur Algebra und Geometrie **35** (1994), no. 2,
K22:29 259–281.
K22:30 [CW96] Robert Connelly and Walter Whiteley, *Second-order rigidity and prestress tensegrity*
K22:31 *frameworks*, SIAM Journal on Discrete Mathematics **9** (1996), no. 3, 453–491.
K22:32 [Dem00] Erik D. Demaine, *Folding and unfolding linkages, paper, and polyhedra*, in: Discrete
K22:33 and Computational Geometry (Jin Akiyama, Mikio Kano, and Masatsugu Urabe,
K22:34 eds.), Revised Papers from the Japan Conference on Discrete and Computational Ge-
K22:35 ometry (Tokyo, Japan), JCDCG 2000, Lecture Notes in Computer Science, vol. 2098,
K22:36 Springer-Verlag, 2001, pp. 113–124.
K22:37 [GSS93] Jack Graver, Brigitte Servatius, and Herman Servatius, *Combinatorial rigidity*, Amer-
K22:38 ican Mathematical Society, Providence, 1993.
K22:39 [Mil68] John Milnor, *Singular points of complex hypersurfaces*, Princeton University Press,
K22:40 1968.
K22:41 [O'R98] Joseph O'Rourke, *Folding and unfolding in computational geometry*, in: Discrete and
K22:42 Computational Geometry (Jin Akiyama, Mikio Kano, and Masatsugu Urabe, eds.),
K22:43 Revised Papers from the Japan Conference on Discrete and Computational Geometry
K22:44 (Tokyo, Japan), JCDCG'98, December 1998, Lecture Notes in Computer Science, vol.
K22:45 1763, Springer-Verlag, 2000, pp. 258–266.
K22:46 [RW81] B. Roth and W. Whiteley, *Tensegrity frameworks*, Transactions of the American Math-
K22:47 ematical Society **265** (1981), no. 2, 419–446.
K22:48 [Str00] Ileana Streinu, *A combinatorial approach to planar non-colliding robot arm motion*
K22:49 *planning*, Proceedings of the 41st Annual Symposium on Foundations of Computer
K22:50 Science (Redondo Beach, California), November 2000, IEEE Computer Society Press,
K22:51 Washington, D.C., 2000, pp. 443–453.
K22:52 [Whi84a] Walter Whiteley, *Infinitesimally rigid polyhedra. I. statics of frameworks*, Transactions
K22:53 of the American Mathematical Society **285** (1984), no. 2, 431–465.
K22:54 [Whi84b] Walter Whiteley, *The projective geometry of rigid frameworks*, in: Finite geometries
K22:55 (Catherine Anne Baker and Lynn Margaret Batten, eds.) Proc. Conf. Winnipeg, 1984,
K22:56 Lecture Notes in Pure and Applied Mathematics, vol. 103, Marcel Dekker, New York–
K22:57 Basel, 1985, pp. 353–370.

[Whi87] Walter Whiteley, *Rigidity and polarity. I. Statics of sheet structures*, Geometriae Dedicata **22** (1987), no. 3, 329–362.

[Whi88] Walter Whiteley, *Infinitesimally rigid polyhedra. II. Modified spherical frameworks*, Transactions of the American Mathematical Society **306** (1988), no. 1, 115–139.

[Whi92] Walter Whiteley, *Matroids and rigid structures*, Matroid applications (Neil White, ed.), Encyclopedia of Mathematics and its Applications, vol. 40, Cambridge University Press, Cambridge, 1992, pp. 1–52.

Appendix A. Constructive Proof of Theorem 8.1

Here we prove another version of Theorem 8.1. We have to make the stronger assumption of *infinitesimal* rigidity, but the proof gives a way to compute δ in terms of ε.

THEOREM A.1. *If a self-touching linkage is infinitesimally rigid, then it is strongly locked.*

PROOF. Let $\mathbf{p}^* = (\mathbf{p}_1^*, \dots, \mathbf{p}_n^*)$ be an infinitesimally rigid self-touching linkage. We can normalize the motions by selecting an edge, say $\mathbf{p}_1\mathbf{p}_2$, and fixing its position: $\mathbf{v}_1 = \mathbf{v}_2 = 0$. Infinitesimal rigidity means that the system $\mathcal{M}$ has only the trivial solution. We apply Lemma 6.2(2) and get a family $\mathcal{M}_1, \mathcal{M}_2, \dots$ of linear systems, all of which have only the trivial solution. Each system $\mathcal{M}_g$ has the form

$$\mathbf{v}_1 = \mathbf{v}_2 = 0 \tag{A.1}$$

$$\mathbf{v}_j \cdot (\mathbf{p}_j^* - \mathbf{p}_i^*) - \mathbf{v}_i \cdot (\mathbf{p}_j^* - \mathbf{p}_i^*) = 0 \tag{A.2}$$

$$-\mathbf{v}_k \cdot (\mathbf{p}_j^* - \mathbf{p}_i^*)^\perp + \alpha \mathbf{v}_i \cdot (\mathbf{p}_j^* - \mathbf{p}_i^*)^\perp + (1-\alpha)\mathbf{v}_j \cdot (\mathbf{p}_j^* - \mathbf{p}_i^*)^\perp \le 0 \tag{A.3}$$

(for all bars i, j and certain triples i, j, k, and certain $\alpha = \alpha_{ijk}$, $0 \le \alpha \le 1$)

LEMMA A.2. *Assume $0 \le \delta \le \varepsilon \le r_1/2$, where r_1 is the minimum positive distance between two vertices or between a vertex and an edge in a given configuration $\mathbf{p}^*$. Let $\mathbf{p}^1$ be a δ-perturbation of $\mathbf{p}^*$:*

$$\|\mathbf{p}^1 - \mathbf{p}^*\| \le \delta,$$

and consider a path $\mathbf{p}(t) \in \mathbb{R}^{2n}$, $0 \le t \le T$, in the configuration space with $\mathbf{p}(0) = \mathbf{p}^1$, with

$$\|\mathbf{p}(t) - \mathbf{p}^*\| < \varepsilon, \text{ for all } 0 \le t \le T$$

Then, for all $\mathbf{p} = \mathbf{p}(t)$, there is a system $\mathcal{M}_g$ in which the equations and inequalities (A.2–A.3) *hold for $\mathbf{p}_i - \mathbf{p}_i^*$ instead of $\mathbf{v}_i$, with a fudge factor $C_1\delta + C_2\varepsilon^2$, where $C_2 = 4$ and C_1 depends only on $\mathbf{p}^*$. More precisely,*

$$-[2\|\mathbf{p}_j^* - \mathbf{p}_i^*\| \cdot \delta + 4\varepsilon^2] \le \ell_{ij} \le 2\|\mathbf{p}_j^* - \mathbf{p}_i^*\| \cdot \delta \tag{A.4}$$

$$\text{with } \ell_{ij} := (\mathbf{p}_j - \mathbf{p}_j^*) \cdot (\mathbf{p}_j^* - \mathbf{p}_i^*) - (\mathbf{p}_i - \mathbf{p}_i^*) \cdot (\mathbf{p}_j^* - \mathbf{p}_i^*),$$

and

$$\begin{aligned} &-(\mathbf{p}_k - \mathbf{p}_k^*) \cdot (\mathbf{p}_j^* - \mathbf{p}_i^*)^\perp \\ &\quad + \alpha(\mathbf{p}_i - \mathbf{p}_i^*) \cdot (\mathbf{p}_j^* - \mathbf{p}_i^*)^\perp + (1-\alpha)(\mathbf{p}_j - \mathbf{p}_j^*) \cdot (\mathbf{p}_j^* - \mathbf{p}_i^*)^\perp \le 4\varepsilon^2. \end{aligned} \tag{A.5}$$

PROOF. The idea of the proof is as follows: By Lemma 3.2, $\mathbf{p}(t)$ must fulfill a set of noncrossing and sidedness conditions. When we write these sidedness condition for $\mathbf{p}$, we get almost (A.5), except that we take the inner product with $(\mathbf{p}_j^* - \mathbf{p}_i^*)^\perp$ instead of $(\mathbf{p}_j - \mathbf{p}_i)^\perp$. For small ε, these two directions are almost parallel, and the

difference is $O(\varepsilon^2)$. For the length-preserving condition there is an additional term of $O(\delta)$ because the length of the bar can change by up to 2δ.

To prove (A.4), we have to bound the difference Δ between

$$(\mathbf{p}_j - \mathbf{p}_i) \cdot (\mathbf{p}_j^* - \mathbf{p}_i^*) = \|\mathbf{p}_j - \mathbf{p}_i\| \cdot \|\mathbf{p}_j^* - \mathbf{p}_i^*\| \cdot \cos\varphi$$

and

$$(\mathbf{p}_j^* - \mathbf{p}_i^*) \cdot (\mathbf{p}_j^* - \mathbf{p}_i^*) = \|\mathbf{p}_j^* - \mathbf{p}_i^*\| \cdot \|\mathbf{p}_j^* - \mathbf{p}_i^*\|,$$

where φ is the angle between $\mathbf{p}_j - \mathbf{p}_i$ and $\mathbf{p}_j^* - \mathbf{p}_i^*$.

$$\Delta = \|\mathbf{p}_j^* - \mathbf{p}_i^*\| \cdot \big(\|\mathbf{p}_j - \mathbf{p}_i\| \cdot \cos\varphi - \|\mathbf{p}_j^* - \mathbf{p}_i^*\|\big).$$

For bounding the right-hand side, we know that $\|\mathbf{p}_j - \mathbf{p}_i\|$ is bounded between $\|\mathbf{p}_j^* - \mathbf{p}_i^*\| \pm 2\delta$, and

$$1 \geq \cos\varphi \geq \sqrt{1 - \left(\frac{2\varepsilon}{\|\mathbf{p}_j^* - \mathbf{p}_i^*\|}\right)^2} \geq 1 - \frac{4\varepsilon^2}{\|\mathbf{p}_j^* - \mathbf{p}_i^*\|^2}.$$

Plugging this in gives the desired relation.

Proof of (A.5): We have

$$\mathbf{p}_k^* = \alpha\mathbf{p}_i^* + (1-\alpha)\mathbf{p}_j^*$$

The corresponding point

$$\bar{\mathbf{p}}_k := \alpha\mathbf{p}_i + (1-\alpha)\mathbf{p}_j$$

lies on the line segment $\mathbf{p}_i\mathbf{p}_j$ and inside the ε-circle around $\mathbf{p}_k$.

We have

$$-\mathbf{p}_k^* \cdot (\mathbf{p}_j^* - \mathbf{p}_i^*)^\perp + \alpha\mathbf{p}_i^* \cdot (\mathbf{p}_j^* - \mathbf{p}_i^*)^\perp + (1-\alpha)\mathbf{p}_j^* \cdot (\mathbf{p}_j^* - \mathbf{p}_i^*)^\perp = 0$$

and

$$-\bar{\mathbf{p}}_k \cdot (\mathbf{p}_j^* - \mathbf{p}_i^*)^\perp + \alpha\mathbf{p}_i \cdot (\mathbf{p}_j^* - \mathbf{p}_i^*)^\perp + (1-\alpha)\mathbf{p}_j \cdot (\mathbf{p}_j^* - \mathbf{p}_i^*)^\perp = 0.$$

The difference between these two terms is almost what we want in (A.5), except that we have to replace $\bar{\mathbf{p}}_k$ by $\mathbf{p}_k$. The point $\mathbf{p}_k$ lies also inside the ε-circle around $\mathbf{p}_k$ and *above* the line segment $\mathbf{p}_i\mathbf{p}_j$. So

$$(\mathbf{p}_k - \bar{\mathbf{p}}_k) \cdot (\mathbf{p}_j^* - \mathbf{p}_i^*)^\perp \geq -2\varepsilon \cdot \|\mathbf{p}_j^* - \mathbf{p}_i^*\| \sin\varphi,$$

where φ is the angle between $\mathbf{p}_j - \mathbf{p}_i$ and $\mathbf{p}_j^* - \mathbf{p}_i^*$. We have

$$\sin\varphi \leq \frac{\varepsilon}{\sqrt{(\|\mathbf{p}_j^* - \mathbf{p}_i^*\|/2)^2 - \varepsilon^2}} \leq \frac{\varepsilon}{\|\mathbf{p}_j^* - \mathbf{p}_i^*\|/2},$$

and this gives

$$(\mathbf{p}_k - \bar{\mathbf{p}}_k) \cdot (\mathbf{p}_j^* - \mathbf{p}_i^*)^\perp \geq -4\varepsilon^2. \qquad \square$$

LEMMA A.3. *Assume that the system $Av = 0$, $Bv \leq 0$ has only the solution $v = 0$. Then for any $\gamma \geq 0$, every solution of $Av = 0$, $Bv \leq \gamma$ (componentwise) has $\|v\| \leq C_3\gamma$, for some constant C_3 depending only on A and B.*

PROOF. The polyhedron $Av = 0$, $Bv \leq 1$ is bounded, and C_3 is the distance of its farthest vertex from the origin. $\square$

K25:01 Finally we prove that $\mathbf{p}^*$ is locked within ε. Let C_3 be a constant for Lemma A.3
K25:02 such that $\|v\| \le C_3\gamma$ holds, for the coefficient matrices A, B of the systems (A.1)
K25:03 and (A.2–A.3), respectively, of all systems $\mathcal{M}_g$. (Each equation of (A.2) is converted
K25:04 into two inequalities and thus contributes two rows to B.) Assume that $\mathbf{p}^1$ and
K25:05 $\mathbf{p} = \mathbf{p}(t)$ are as in Lemma A.2 with $\varepsilon := 1/(3C_2C_3)$ and $\delta := 1/(9C_1C_2C_3^2) = \frac{\varepsilon}{3C_1C_3}$.
K25:06 By choosing a larger constant C_3 if necessary we can assure that δ and ε satisfy the
K25:07 assumptions of Lemma A.2, and by choosing a larger constant C_2 we can ensure
K25:08 that ε is smaller than any given desired value. We can also assume that the motion
K25:09 $\mathbf{p}(t)$ leaves the edge $\mathbf{p}_1\mathbf{p}_2$ stationary, i. e., $\mathbf{p}_1 - \mathbf{p}_1^* = \mathbf{p}_2 - \mathbf{p}_2^* = 0$. Then we know
K25:10 that $v = \mathbf{p} - \mathbf{p}^*$ fulfills $Av = 0$, $Bv \le \gamma$ with

K25:11 $$\gamma = C_1\delta + C_2\varepsilon^2 = \frac{2}{9} \cdot \frac{1}{C_2C_3^2}$$

K25:12 and, by Lemma A.3, this implies $\|\mathbf{p}_i - \mathbf{p}_i^*\| \le C_3\gamma = \frac{2}{9} \cdot \frac{1}{C_2C_3} = \frac{2}{3}\varepsilon$.
K25:13 It follows that $\mathbf{p}$ cannot possibly reach any position with

K25:14 $$\tfrac{2}{3}\varepsilon < \max_i \|\mathbf{p}_i - \mathbf{p}_i^*\| \le \varepsilon.$$

K25:15 Thus each point $\mathbf{p}_i$ is confined within a disk of radius $\frac{2}{3}\varepsilon$ around $\mathbf{p}_i^*$. □

K25:16 To compute the value of δ for a given ε, we have to know the constants C_1,
K25:17 C_2, C_3, and r_1. We have $C_2 = 4$ and $C_1 = 2D_{\max}$, where $D_{\max}$ is the length of
K25:18 the longest bar. These are geometric quantities of the configuration. The constant
K25:19 C_3 is harder to compute. We can approximate it by computing the axes-parallel
K25:20 bounding box of the polytope $Av = 0$, $Bv \le 1$, solving $O(n)$ linear programming
K25:21 problems. The size of this polytope measures how "rigid" the linkage is, in terms of
K25:22 sensitivity to tolerances in the edge lengths. Edges that are almost parallel where
K25:23 they meet will in general lead to a large polytope.
K25:24 If we draw the tree in Figure 1(c) symmetrically and put $OA = 1$ and $OB = 1/3$
K25:25 (in the notation of Figure 11b), we get $C_1 = 2$ and $C_3 \le 626$, using the norm (3.1).
K25:26 By plugging these values into the formulas, one obtains that any δ-perturbation
K25:27 of the tree is locked within ε, for $\delta = 3 \times 10^{-8}$ and $\varepsilon = 0.0001$. One can slightly
K25:28 improve these formulas by balancing δ and ε in the derivation. A direct, but tedious
K25:29 proof reveals that the tree is locked for $\delta = 0.00005$, but unlocked for $\delta = 0.001$.

K25:30 Department of Mathematics, Cornell University, Ithaca, NY 14853, U.S.A.
K25:31 *E-mail address*: connelly@math.cornell.edu

K25:32 MIT Laboratory for Computer Science, 200 Technology Square, Cambridge, MA 02139,
K25:33 U.S.A.
K25:34 *E-mail address*: edemaine@mit.edu

K25:35 Institut für Informatik, Freie Universität Berlin, Takustrasse 9, D-14195 Berlin,
K25:36 Germany
K25:37 *E-mail address*: rote@inf.fu-berlin.de